Oxygen Activation (Hagishi, O., Ed.) p 559, Academic Press, New York.
Haldane, J. S., & Smith, L. (1896) *J. Physiol. 20*, 497.
Hanson, L. K., Eaton, W. A., Sligar, S. G., Gunsalus, I. C., Gouterman, M., & Connell, C. R. (1976) *J. Am. Chem. Soc. 98*, 2672.
Hollenberg, P. F., & Hager, L. P. (1973) *J. Biol. Chem. 248*, 2630.
Kitagawa, T., Abe, M. Kyogoku, Y., Ogoshi, H., Sugimoto, H., & Yoshida, Z. (1977) *Chem. Phys. Lett. 48*, 55.
Kitagawa, T., Abe, M., & Ogoshi, H. (1978) *J. Chem. Phys. 69*, 4516.
Krejcarek, G. E., Bryant, R. G., Smith, R. J., & Hager, L. P. (1976) *Biochemistry 15*, 2508.
Makino, R., Chiang, R., & Hager, L. P. (1976) *Biochemistry 15*, 4748.
Morris, D. R., & Hager, L. P. (1966) *J. Biol. Chem. 241*, 1763.
Ozaki, Y., Kitagawa, T., Shimada, H., Iizuka, T., & Ishimura, Y. (1976) *J. Biochem. (Tokyo) 80*, 1447.
Rakshit, G., & Spiro, T. G. (1974) *Biochemistry 13*, 5317.
Spiro, T. G., & Strekas, T. C. (1974) *J. Am. Chem. Soc. 96*, 338.
Spiro, T. G., & Burke, J. M. (1976) *J. Am. Chem. Soc. 98*, 5482.
Stein, P., Burke, J. M., & Spiro, T. G. (1975) *J. Am. Chem. Soc. 97*, 2304.
Sunder, S., & Bernstein, H. J. (1976) *J. Raman Spectrosc. 5*, 351.
Thomas, J. A., Morris, D. R., & Hager, L. P. (1970) *J. Biol. Chem. 245*, 3129.

Proton Coupling in the Cytochrome P-450 Spin and Redox Equilibria†

Stephen G. Sligar* and I. C. Gunsalus

ABSTRACT: Ferric bacterial cytochrome P-450 is known to exist as a mixture of high-spin ($S = 5/2$) and low-spin ($S = 1/2$) configurations of the heme iron d-shell electrons. This equilibrium between the two forms of P-450 has been shown to control both substrate affinity and the observed redox potential. Room temperature binding of a solvent-exchangeable proton to high-spin, substrate-free P-450 occurs with pK = 6.5, while camphor association shifts this equilibrium to a pK of 5.8. No H^+ ligation to the low-spin forms of P-450 is observed. Proton coupling is also observed in the reduction of camphor-bound, high-spin ferric P-450. Analysis of these structures by a four-state, free-energy coupling model yields pKs of 5.8 and 8.0 for H^+ binding respectively to Fe^{3+} and Fe^{2+} P-450 and inherent electrode potentials of −106 and −238 mV for the oxidation/reduction of protonated and unprotonated protein. Analysis of the free-energy interaction diagram yields the standard state potential $E^{\circ\prime} = -173$ mV at pH 7 for camphor-bound material. Proton modulation of the putidaredoxin–cytochrome P-450 electron transfer in a stabilized dienzyme complex is quantitated by stopped-flow spectrophotometry. Protonation of the multiprotein complex is seen to occur on cytochrome reduction–redoxin oxidation with pK = 5.8, indicating that, at pH 7, there is little equilibration with solvent protons. The possibility of concerted H^+/e^- transfer during P-450-catalyzed, mixed function oxidation is discussed.

Cytochrome P-450 is the terminal mixed function oxidase of a short flavoprotein and iron–sulfur protein electron transport chain linking pyridine nucleotide oxidation, with O_2 reduction and concomitant substrate oxygenation through the production of water and hydroxylated substrate. Enzymatic hydroxylations are found ubiquitously in living species as a means of xenobiotic and steroid metabolism and exhibit varying degrees of substrate specificity. The most commonly studied hydroxylases are the hepatic microsomal P-450 responsible for general detoxification and hydrocarbon solubilizations (Orrenius & Ernster, 1974), the adrendal mitochondrial enzymes active in the conversion of cholesterol to the various steroid hormones (Hamberg et al., 1974), and the camphor 5-*exo*-hydroxylase from the soil bacterium *Pseudomonas putida* (Gunsalus et al., 1975). This last system, discovered and investigated in detail by the Gunsalus laboratory (Hedegaard & Gunsalus, 1965), offers the outstanding advantages of high purity and yield necessary for precise, quantitative biochemistry, and will be the enzyme used in the investigations reported herein.

The two central areas of P-450 mechanism which have been under active investigation in our laboratories center on the chemistry of O_2 bond cleavage/substrate oxygenation and the physical biochemistry of the redox transfer events leading from flavoprotein dehydrogenation, through the iron–sulfur protein, to the cytochrome. This area provides a molecular description of the regulation and control of redox equilibria in cytochrome P-450 through substrate ligation (Sligar & Gunsalus, 1976) and the interconversion of the d^5-ferric heme iron from a low-spin ($S = 1/2$) to high-spin ($S = 5/2$) configuration (Sligar, 1976). This communication adds to the interacting equilibria the binding of protons to the cytochrome to illustrate an ionic control of spin and substrate binding, thus suggesting a possible concerted electron/proton transfer event within the

† From the Department of Molecular Biophysics and Biochemistry, Yale University, New Haven, Connecticut 06520 (S.G.S.), and the Department of Biochemistry, University of Illinois, Urbana, Illinois 61801 (I.C.G.).
Received August 17, 1978; revised manuscript received March 2, 1979. Supported by grants from the National Institutes of Health (GM 24976, GM 18051) and the Biomedical Research Support (RR-07015).

0006-2960/79/0418-2290$01.00/0

redoxin–cytochrome dienzyme complex.

The early cryogenic electron paramagnetic resonance experiments by Tsai in 1970 (Tsai et al., 1970) noted that substrate binding induced a change in the spin state of the five iron d-shell electrons from totally low-spin ($S = 1/2$) to a mixture of low- and high-spin ($S = 5/2$) configurations. Substrate association was found also to alter the redox potential of P-450 from roughly −300 mV to −170 mV on camphor ligation. The interaction of substrate and redox equilibria was analyzed in fundamental thermodynamic terms (Sligar & Gunsalus, 1976), demonstrating the conservation of Gibbs free energy in the asymmetric substrate disassociation constants and alterations in electrode potentials of the heme protein. Attention to the spin state of the cytochrome revealed in the bacterial P-450 system, and in whole hepatic microsomal preparations, that temperature variations of the sample produce reversible type I spectral changes of the P-450 heme chromophore (Sligar, 1976; Lang et al., 1977; Pierson & Cinti, 1977). Subsequent analysis by temperature-induced difference spectroscopy allowed precise quantitation of both the equilibrium constant for the $S = 1/2$ to $S = 5/2$ spin equilibrium at any temperature and the thermodynamically relevant enthalpy and entropy for the process (Sligar, 1976; Cinti et al., 1979).[1] Straightforward extension to include the P-450 electrode potentials in the various states gave a thermodynamically complete free-energy coupling model for the interaction of spin, substrate, and redox equilibria and illustrated the importance of the iron d-electron distribution in controlling both electron transfer from redoxin and substrate affinity (Sligar, 1976).

Inasmuch as the overall oxygenase stochiometry requires two protons as well as two electrons, in this communication we examine the thermodynamic coupling of proton ligation to the spin and redox equilibria of bacterial cytochrome P-450.

Materials and Methods

Cytochrome P450 was isolated from *Pseudomanas putida* strain PpG786 (ATCC 29607) essentially as described (Gunsalus & Wagner, 1978), except for preparations at Yale where fermentation was carried out in a 30-L air-sparged carboy, and all desalting steps were by column rather than continuous filtration. Cytochrome purity quantitated by the A_{390nm}/A_{280nm} ratio was greater than 1.35 in all cases. All chemicals were of the highest purity reagent grade obtained from standard suppliers.

Absolute spin equilibrium constants were determined by the regression analysis previously described (Sligar, 1976). Redox potentials were quantitated by the dye photoreduction procedure (Sligar & Gunsalus, 1974) by using recrystallized Safranine T ($E_0 = -289$ mV) (Sober, 1970). All optical measurements were conducted on a Cary 219 UV–visible spectrophotometer with wavelength and time programmers that was generously purchased by the Yale Department of Molecular Biophysics and Biochemistry or on a McPherson EU700 series spectrophotometer. Cell temperatures were continuously recorded by thermistor and digital multimeter. Stopped-flow experiments utilized an Amino-Chance module with 1.5-ms dead time and a single wavelength optical bench consisting of tungsten–halogen lamp, monochromator, and 1P28 phototube. Transmitted light intensity was converted to absorbance units on-line with an Analog Devices 755 log amplifier and recorded on a Textronix 5000 series dual differential storage oscilloscope.

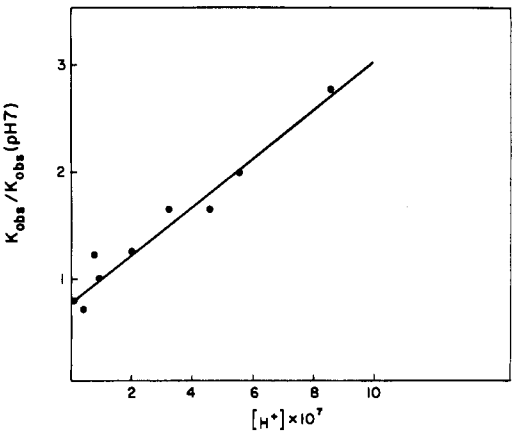

FIGURE 1: Proton dependence of the m° spin equilibrium. The observed total equilibrium constant for the interconversion of ferric substrate-free P-450 (m°) between low spin, m^{os}_{ls}, and unprotonated, m^{o}_{hs}, and protonated, Hm^{o}_{hs}, forms is plotted as a function of hydrogen ion concentration. K_{obsd}(pH 7) is the observed equilibrium constant at pH 7. K_{obsd}(pH 7) = 0.086 (Sligar, 1976). Cytochrome P-450 is 10 μM in 50 mM potassium phosphate buffer containing 120 mM KCl.

Results

(1) Proton Coupling to the m° Spin Equilibrium.[2] Cytochrome P-450 both with (m^{os}) and without (m^{o}) substrate bound has been shown to exist as a temperature-dependent mixture of low- (m_{ls}) and high- (m_{hs}) spin forms. When the equilibrium constant for this process (K_{obsd}) is quantitated as a function of the total hydrogen ion concentration, the results shown in Figure 1 are obtained. In general, the modulation of any internal equilibrium constant by the asymmetric binding of a ligand can be described in terms of a four-state free-energy coupling model (Sligar & Gunsalus, 1974; Weber, 1975). In this case, the four states of substrate-free cytochrome P-450 are: m^{o}_{ls}, low spin unprotonated; m^{o}_{hs}, high spin unprotonated; Hm^{o}_{ls}, low spin protonated; and Hm^{o}_{hs}, high spin protonated. It is entirely possible, however, for the proton to bind in only one spin-state configuration, in which case the corresponding microscopic disassociation constant for ligation to the other state would be infinite. In this case we have the equilibria:

$$m^{o}_{ls} \overset{K_1}{\leftrightarrow} m^{o}_{hs} \underset{\pm H^+}{\overset{K_2}{\leftrightarrow}} Hm^{o}_{hs}$$

Such cases can be uncovered by plotting the data as in Figure 1. Here K_1 is the microscopic equilibrium constant for the interconversion of P-450 between low- and high-spin forms in the absence of H^+

$$K_1 = \frac{[m^{o}_{hs}]}{[m^{o}_{ls}]}$$

and K_2 is the microscopic disassociation constant for proton ligation to m^{o}_{hs}:

$$K_2 = \frac{[H^+][m^{o}_{hs}]}{[Hm^{o}_{hs}]}$$

If H^+ can associate only to the high-spin form of the cytochrome, the observed equilibrium constant K_{obsd} is given by

[1] The ionization dependence of camphor binding and spin conversion of the complex between cytochrome P-450 and camphor were elegantly documented by Lang et al. (1977). See also Lang & Debey (1979) and Lang et al. (1979).

[2] Bacterial cytochrome P-450 is abbreviated cytochrome m for monoxygenase following recognized usage. Superscripts indicate oxidation state (m^{o}, oxidized, ferric; m^{r}, reduced, ferrous) and substrate bound (m^{os} and m^{rs}, respectively) forms. High-spin and low-spin states are indicated by subscripts hs and ls, respectively. Other abbreviation: Pd, putidaredoxin.

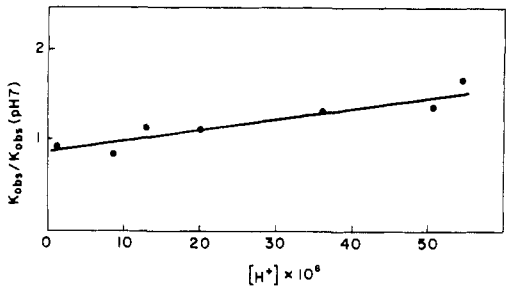

FIGURE 2: Proton dependence of the m^{os} spin equilibrium. Conditions and terminology are as in Figure 1, except that the cytochrome is saturated with camphor (400 μM). K_{obsd}(pH 7) = 15 (Sligar, 1976).

total high-spin concentration divided by total amount of low-spin cytochrome

$$K_{obsd} = \frac{[m^{o}_{hs}] + [Hm^{o}_{hs}]}{[m^{o}_{ls}]} = K_1\left[1 + \frac{[H^+]}{K_2}\right]$$

predicting a straight line when K_{obsd} is plotted against $[H^+]$ with slope $1/K_2$ and intercept K_1. If, on the other hand, protons also coupled to m^{o}_{ls}, one would expect to see a saturation behavior in K_{obsd} at high H^+ concentrations with the limiting value of K_{obsd} being the microscopic spin equilibrium constant for the completely protonated form of P-450. As can be readily seen from Figure 1, over the titrated pH range, which is limited by protein stability, K_{obsd} rises linearly with $[H^+]$ and no evidence of saturation exists. We therefore conclude that the pK for H^+ binding to m^{o}_{ls} at room temperature must be less than five with protons coupling primarily to the high-spin form of P-450. The values of slope and intercept together with the above equations yield values of K_{obsd}/K_{obsd}(pH 7) = 0.31 and $K_2 = 3.3 \times 10^{-7}$ (pK_2 = 6.5).

(2) *Proton Coupling to the m^{os} Spin Equilibrium.* The total spin equilibrium constant, K_{obsd}, as a function of hydrogen ion concentration can likewise be quantitated for substrate-bound P-450, with entirely identical methods of analysis. These results, shown in Figure 2, show an analogous proton modulation of the m^{os} spin equilibrium with H^+ again coupling only to the high spin form of the cytochrome:

$$m^{os}_{ls} \overset{K_1}{\leftrightarrow} m^{os}_{hs} \overset{K_2}{\underset{\pm H^+}{\leftrightarrow}} Hm^{os}_{hs}$$

From Figure 2 and the analogous equations presented earlier, one derives values K_{obsd}/K_{obsd}(pH 7) = 0.93 and $K_2 = 1.58 \times 10^{-6}$ (pK_2 = 5.8). A larger absolute value of K_1 is measured with camphor bound (Sligar, 1976) and corresponds to a shift in the P-450 spin state from predominantly low spin for m^{o} to predominantly high spin for m^{os}. Of primary interest in this communication is the shift in pK for protonation of the high-spin state from pK = 6.5 for m^{o}_{hs} to pK = 5.8 for m^{os}_{hs}.

(3) *Proton Coupling to the Cytochrome P-450 Redox Potential.* Inasmuch as the P-450 spin, substrate binding, and redox equilibria were shown to constitute a three-dimensional interacting system via Gibbs free-energy linkages (Sligar, 1976), we were anxious to explore the possibility of proton coupling to the cytochrome P-450 redox potential. Since the addition of proton binding to the above equilibria constitutes a $2^4 = 16$ state system with a correspondingly large number of independent equilibrium constants, we have chosen to examine in this communication only the coupling of H^+ to the substrate-bound form of the cytochrome.

Interaction of proton and electron during the oxidation–reduction of P-450 is described energetically by Scheme I. Since ferrous P-450 is in a complete high-spin $S = 2$ con-

Scheme I

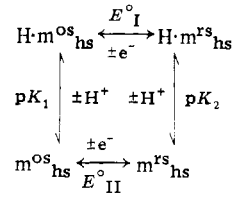

figuration (Sharrock et al., 1973; Champion et al., 1975), only four states contribute: m^{os}_{hs}, Hm^{os}_{hs}, m^{rs}_{hs}, and Hm^{rs}_{hs}. pK_1 and pK_2 correspond to the protonation of m^{os}_{hs} and m^{rs}_{hs}, respectively, while E°_{I} and E°_{II} are the formal microscopic electrode potentials for the oxidation–reduction of protonated and unprotonated high-spin cytochrome P-450. These four equilibria constitute a thermodynamically closed system with conservation of the Gibbs free-energy state function as one proceeds around the diagram shown in Scheme I.

Defining the microscopic potential, E_{II}, by

$$E_{II} = E^{\circ}_{II} + \frac{RT}{nF} \ln \frac{[m^{os}_{hs}]}{[m^{rs}_{hs}]}$$

and the proton equilibrium constants K_1 and K_2 by

$$K_1 = \frac{[H^+][m^{rs}_{hs}]}{[Hm^{rs}_{hs}]} \qquad K_2 = \frac{[H^+][m^{os}_{hs}]}{[Hm^{rs}_{hs}]}$$

One can easily show that

$$E_{II} = E^{\circ}_{II} + \frac{RT}{nF} \ln \frac{[m^{os}_{T}]}{[m^{rs}_{T}]} - \frac{RT}{nF} \ln \left[\frac{1 + \dfrac{[H^+]}{K_2}}{1 + \dfrac{[H^+]}{K_1}}\right]$$

where $[m^{os}_{T}] = [m^{os}_{hs}] + [Hm^{os}_{hs}]$ is the total concentration of ferric high-spin P-450 and $[m^{rs}_{T}] = [m^{rs}_{hs}] + [Hm^{rs}_{hs}] = [m^{rs}_{hs}](1 + [H^+]/K_1)$ is the total concentration of ferrous P-450. In this analysis, we have neglected the state m^{os}_{ls} since it has previously been shown (Sligar, 1976) that substrate-bound cytochrome is greater than 95% high spin. If one had considered the other microscopic electrode potential, E°_{I}, an analogous expression could be derived

$$E_I = E^{\circ}_{I} + \frac{RT}{nF} \ln \frac{[m^{os}_{T}]}{[m^{rs}_{T}]} + \frac{RT}{nF} \ln \left[\frac{1 + (K_1/[H^+])}{1 + (K_2/[H^+])}\right]$$

where E_I and E_{II} are related by the free-energy coupling of the proton association

$$E_{II} - E_I = E^{\circ}_{II} - E^{\circ}_{I} - \frac{RT}{nF} \ln \left[\frac{K_1}{K_2}\right]$$

At equilibrium the observed system potential, E_{obsd}, follows both processes; for example:

$$E_{obsd} = E^{\circ}_{I} + \frac{RT}{nF} \ln \left(\frac{[H^+] + K_1}{[H^+] + K_2}\right)$$

Figure 3 shows the results of a redox titration of cytochrome P-450 with the observed system potential plotted as a function of the hydrogen ion concentration. It is obvious that there exists a proton ligation coupled to the redox state of cytochrome P-450. The smooth curve through the data in Figure 3 is the best regression fit for the two parameters, E°_{I} and K_1, and yields values for the fundamental microscopic parameters of $E^{\circ}_{I} = -106$ mV, $E^{\circ}_{II} = -238$ mV and pK_1 = 8 with pK_2 = 5.8 being supplied by spin-state analysis (Figure 2). This

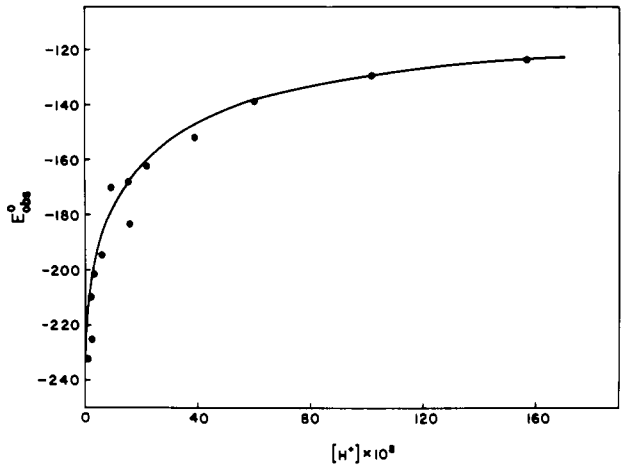

FIGURE 3: Proton dependence of the m^{os} redox potential. The observed redox potential of camphor-saturated P-450 is quantitated as a function of hydrogen ion concentration. Potentials are measured by the dye photoreduction method (Sligar & Gunsalus, 1974). The four-state system has four equilibrium constants, with only three being independent due to conservation of Gibbs free energy (see text). pK_2 = 5.8 is taken from Figure 2, yielding two independent parameters for the data shown here. The solid line is the least-squares regression line with the corresponding values of pK_1, E°_{I}, and E°_{II} described in the text.

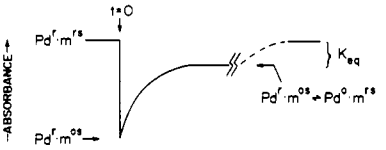

FIGURE 4: Oxidation kinetics of reduced putidaredoxin. A representative stopped-flow recording of putidaredoxin (Pd)–P-450 electron transfer is shown. Pd^r is contained in one syringe at 40 μM with a tenfold excess of dithionite in 50 mM potassium phosphate buffer, 120 mM KCl, pH 7.0. Oxidized, substrate-bound P-450 is contained in the second syringe in 50 mM potassium phosphate buffer, 120 mM KCl. Solutions are made and transferred anerobically by repeated application of vacuum and exposure to nitrogen prepurified over BASF catalyst (Kontes Glass, NJ). These concentrations of redoxin and cytochrome are more than sufficient to guarantee greater than 98% complex formed in an order of magnitude less than the dead time of the instrument (Sligar & Gunsalus, 1974). Reoxidation is followed to a level plateau extending from ~100 to 900 ms. Slow reduction of the cytochrome by the excess dithionite occurs on a time scale of seconds providing a direct, internally consistent, quantitation of K_{eq}.

shift in pK for the cytochrome upon reduction (pK = 5.8 to pK = 8.0) indicates that at neutral pH the system moves predominantly from the state m^{os}_{hs} to Hm^{rs}_{hs}, thus abstracting a proton from the solution concomitant with electron uptake.

(4) Proton Coupling to Putidaredoxin–P-450 Electron Transfer in a Dienzyme Complex. It has been well documented (Sligar & Gunsalus, 1974, 1976; Pederson & Gunsalus, 1976; Debey et al., 1977) that electron transfer from the physiological donor putidaredoxin (abbreviated Pd, with superscripts indicating oxidation state: Pd^o, oxidized; Pd^r, one electron reduced) to the cytochrome occurs through the formation of a dienzyme complex between iron–sulfur protein and P-450. Inasmuch as a net proton uptake is seen on the ferric–ferrous reduction of isolated cytochrome P-450, it is of prime interest to understand the role of hydrogen ions in mediating the putidaredoxin–P-450 redox transfer in the dienzyme complex. Denoting reduced and oxidized putidaredoxin by Pd^r and Pd^o respectively, the equilibrium constant for transfer in the complex $Pd^r \cdot m^{os} \rightleftarrows Pd^o \cdot m^{rs}$ can conveniently be measured by stopped-flow spectrophotometry. The nature of the experimental determination of this equilibrium constant can be understood by reference to Figure 4. As described in

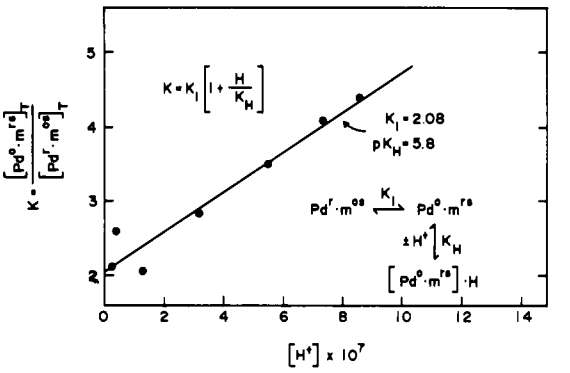

FIGURE 5: Proton coupling in Pd–P-450 electron transfer. The equilibrium constant, K, derived as described in Figure 4, is plotted as a function of hydrogen ion concentration. The data shown correspond to a proton uptake by the $[Pd^o \cdot m^{rs}]$ complex with pK = 5.8.

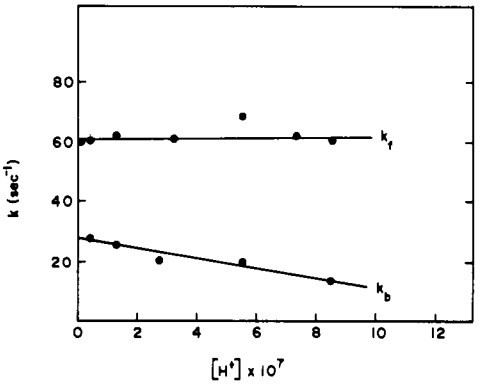

FIGURE 6: Proton dependence of the Pd ↔ P-450 electron transfer rates. Rate constants derived from the time-dependent exponential reaction shown schematically in Figure 4 are plotted as a function of hydrogen ion concentration.

the legend to Figure 4, the presence of excess dithionite in the Pd^r syringe and its slow rate for reducing Pd and P-450 allow internal standardization and direct measurement of both the equilibrium constant, K_{eq}, and the relaxation rate to equilibrium.

Quantitation of K_{eq} as a function of hydrogen ion concentration yields the results presented in Figure 5. Following the general scheme discussed earlier, the linear behavior of K_{eq} vs. $[H^+]$ indicates the scheme shown on the figure insert where the dienzyme complex binds a single solvent-exchangeable proton with a pK = 5.8. This pK, however, is to be contrasted with the results of Figure 3 where the isolated cytochrome is seen to uptake a proton upon reduction at neutral pH. Here a pK of 5.8 shows that at pH 7 there is no net coupling between redox transfer in the dienzyme complex and the bulk solvent protons. The individual forward and back rate constants k_f and k_b for electron donation from putidaredoxin to P-450 are shown as a function of $[H^+]$ in Figure 6, where it is clear that proton dissociation is rate limiting in the control of electron flow in the dienzyme complex between redoxin and cytochrome.

Discussion

Cytochrome P-450 is known to exist as a mixture of low- and high-spin forms which are temperature interconvertible (Sligar, 1976; Lang et al., 1977; Pierson & Cinti, 1977; Cinti et al., 1979). The precise value of spin equilibrium constant was also shown to dictate the absolute electrode potential of P-450, there being an inherent potential for reducing high-spin P-450 heme iron, and a correspondingly lower potential for oxidation/reduction of low-spin cytochrome (Sligar, 1976).

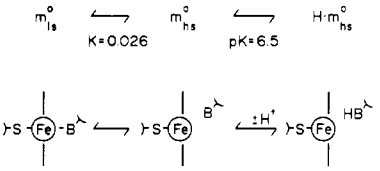

FIGURE 7: Hypothetical model for proton uptake by high-spin substrate-free P-450 (m^{o}_{hs}). Six-coordinated low-spin P-450 contains a proximal (S) and distal (B) axial ligand. Removal of B from the heme iron, corresponding to a shift to the high-spin configuration, allows proton binding to the free base $B + H^{+} \leftrightarrow BH$. See text.

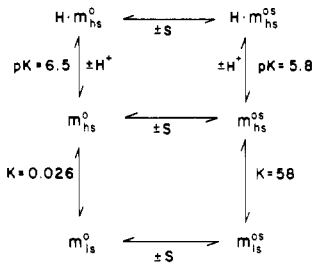

FIGURE 8: Proton, spin, and substrate states of cytochrome P-450. See text.

The results presented herein extend the multidimensional, free-energy coupling model of spin, redox potential, and substrate ligation to include modulation of these equilibria through hydrogen ion binding.

Substrate-free P-450 (m^{o}) has an overall equilibrium constant $K_{obsd} = 0.086$ at pH 7 for the process $m^{o}_{ls} \leftrightarrow m^{o}_{hs}$ (Sligar, 1976). Variation of the H^{+} concentration, Figure 1, shows this overall equilibrium to be composed of two distinct processes: a "bare" spin equilibrium constant K_1, $m^{o}_{ls} \leftrightarrow m^{o}_{hs}$; and a protonation constant, $pK_2 = -\log K_2 = 6.5$. The linearity of the data in Figure 1, with the absence of a saturable proton site over the pH range, compatible with enzyme stability, indicates that H^{+} binding occurs only in the high-spin form of the cytochrome.

The absolute configuration of the d^5 electrons in ferric heme proteins is dictated by the strength of the ligand field at the iron center. Six-coordinated heme (four in-plane pyrrole nitrogens and two axial ligands) with two strong field axial components generate sufficient crystal field to force the d^5 system into the low-spin $S = 1/2$ state, as in this case it is much more energetically favorable to spin-pair than populate the upper levels. With the weak crystal field generated in a five-coordinated heme (only one axial ligand), it becomes more likely to populate all orbitals with a minimum of spin-pairing, thus generating an $S = 5/2$, high-spin iron. The dogma of high–low-spin interconversion being linked to a change in macromolecular structure through reversible binding of the 6th heme ligand has been established and is consistent in many cases with the measured thermodynamic parameters for the process (Sligar, 1976; Iizuka & Yonetani, 1970). In this case, it is natural to assign the high-spin H^{+} coupling site to proton binding to the free distal base as shown in Figure 7. The derived pK for the process ($pK = 6.5$ for $m^{o}_{hs} \leftrightarrow H{\cdot}m^{o}_{hs}$) suggests the possibility of an imidazole group for this ligand, although, since the proximity of charged or hydrophobic amino acids to the proton binding site can drastically alter the microscopic pK, such assignment cannot be absolute. It is also possible that the observed proton uptake on conversion to high spin does not directly involve an axial heme ligand but rather is coupled to a generalized conformational change in analogy with the salt proton of hemoglobin. Similar arguments are applicable for substrate bound P-450 (m^{os}) with a slightly different pK for proton association.

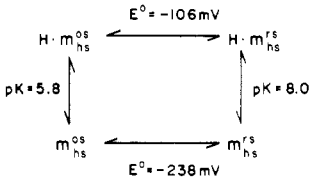

FIGURE 9: Proton and electron states of cytochrome P-450. See text.

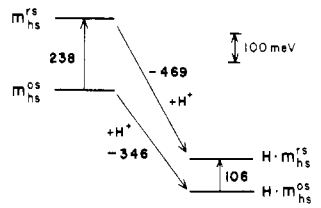

FIGURE 10: Proton modulation of the cytochrome P-450 redox potential. A free-energy diagram of the electron and proton levels drawn to the scale shown. (1 eV = 23 kcal/mol). Redox potentials are converted to Gibbs energies via the relation $\Delta G = -nF\Delta E$.

Figure 8 summarizes schematically the coupling of protons to the spin and substrate equilibria of cytochrome P-450. Each of the states m^{o}_{ls} (high spin $S = 5/2$) and $H{\cdot}m^{o}_{hs}$ (protonated high spin) is linked to the corresponding substrate bound states (m^{os}_{ls}, m^{os}_{hs}, and $H{\cdot}m^{os}_{hs}$) by a camphor-binding reaction. Such a diagram can be considered in energetic terms (Sligar & Gunsalus, 1976). In particular, the changes from $pK = 6.5$ for substrate-free cytochrome to $pK = 5.8$ for camphor-complexed material must be translated into a corresponding asymmetry in the binding of substrate to the protonated and unprotonated high-spin forms (Weber, 1975). Independent and elegant measurements of the actual camphor binding constants for m^{o}_{hs} and $H{\cdot}m^{o}_{hs}$ (Lang et al., 1977) confirm an asymmetry in equilibrium energies, and also point out a variation in the enthalpy of the spin transition in mixed solvents as a function of hydrogen ion activity. Such information suggests a more complex description of the H^{+} equilibria in P-450 which is under current active investigation by P. Debey, P. Douzou, and R. Lang in Paris.

Extension of this analysis to the proton modulation of the substrate-bound redox equilibria is summarized in Scheme I and Figure 9. Oxidized cytochrome protonates with $pK = 5.8$, while reduction of the heme iron shifts this H^{+} equilibria constant to $pK = 8.0$. This asymmetry in proton ligation is directly related by free energy conservation to a nonequivalence of electrode potential, with values $E° = -106$ mV for the oxidation/reduction of protonated P-450 and $E° = -238$ mV for the redox couple of unprotonated cytochrome. At pH 7 one deals primarily with the states m^{os}_{hs} and $H{\cdot}m^{rs}_{hs}$ and, hence, there is a single H^{+} uptake coupled to electron flow. Trivial solution of the four-state equilibrium constants of Figure 9 allows direct calculation of the observed cytochrome electrode potential at any pH, yielding, for example, $E°' = -173$ mV at pH 7 (Sligar & Gunsalus, 1976). If desired, the asymmetric interaction of H^{+} ligation in the control of cytochrome potential can be cast into a scaled energy diagram, Figure 10, similar to that for substrate association (Sligar, 1976). In this context, the larger binding free energy (−469 meV, −45.3 kJ/mol) of H^{+} to ferrous P-450 over the ferric (−346 meV, −33.4 kJ/mol) lowers the Gibbs redox energy difference from 238 meV (23.0 kJ/mol) to 106 meV (10.2 kJ/mol), thus controlling electron input from the physiological, pyridine-nucleotide-linked redox chain.

Studies of interacting equilibria of isolated components of the camphor monoxygenase system provide the basis for understanding the modulation and control of the detailed

microscopic processes involved in mixed function oxidation. Physiological electron flow between redoxin (Pd) and cytochrome, however, is known to occur in a dienzyme complex (Sligar & Gunsalus, 1976; Pederson & Gunsalus, 1975; Debey et al., 1977; Bon Hoa et al., 1978). Hence, it becomes crucial to examine proton coupling to the Pd·P-450 dienzyme complex during redox transfer. The results presented in Figure 2 unambiguously show a single H^+ binding to the oxidized redoxin-reduced cytochrome ($Pd^o{\cdot}m^n$) complex. A pK = 5.8, however, implies that at pH 7 there is only weak coupling between the solvent protons and the transfer of electrons between redoxin and cytochrome. Since isolated P-450 shows a strong pH coupling with a single H^+ uptake at pH 7, either the association of the protein components drastically modulates the relevant pKs of the oxidized and reduced components or there is a possibility of concerted H^+ transfer in the dienzyme complext not coupled to the external pH of the medium. Preliminary measurements of redoxin–cytochrome association by using fluorescein-labeled P-450 (Sligar & Gunsalus, 1974) suggest a weak or absence of H^+ coupling to the actual multiprotein association equilibria. If borne out by further studies this would suggest a concerted proton transfer between redoxin and cytochrome in the two-protein complex system.

In summary, the results presented in this communication demonstrate the importance of H^+ in monoxygenation reactions. Since reductive cleavage of the O_2 bond results in both electron and proton transfer to an oxygen atom, continued study of H^+ linked equilibria will further illuminate the ordering and importance of proton and general ion reactions.

Acknowledgments

Deep gratitude is owed to the Department of Molecular Biophysics and Biochemistry at Yale for the purchase of the Cary 219 spectrophotometer and to Dr. N. Ornston for the gift of a pH meter. Our collaborative efforts are greatly aided by the input from Drs. Pierre Douzou, Pascale Debey, and Rinhardt Lang at the Institute de Biologie Physico Chimique in Paris. The technical assistance of John Burt, M. J. Namtredt, and the protein purification group at Illinois is gratefully acknowledged.

References

Bon Hoa, G. H., Begard, E., Debey, P., & Gunsalus, I. C. (1978) *Biochemistry 17*, 2835.

Champion, P., Lipscomb, J. D., Munck, E., Debrunner, P., & Gunsalus, I. C. (1975) *Biochemistry 14*, 4151.

Cinti, D., Sligar, S. G., Gibson, G. G., & Schenkman, J. B. (1979) *Biochemistry 18*, 36.

Debey, P., Bon Hoa, G. H., & Gunsalus, I. C. (1977) *Croat. Chem. Acta 49*, 309.

Gunsalus, I. C., & Wagner, G. (1978) *Methods Enzymol. 52*, 166.

Gunsalus, I. C., Pederson, T., & Sligar, S. G. (1975) *Annu. Rev. Biochem. 44*, 377.

Hamberg, M., Samuelsson, B., Ingemar, B., & Danielsson, H. (1974) in *Molecular Mechanisms of Oxygen Metabolism* (Hayaish, O., Ed.) p 30, Academic Press, New York.

Hedegaard, J., & Gunsalus, I. C. (1965) *J. Biol. Chem. 240*, 4038.

Iizuka, T., & Yonetani, T. (1970) *Adv. Biophys. 1*, 157.

Lang, R., & Debey, P. (1979) *Eur. J. Biochem. 70* (in press).

Lang, R., Bon Hoa, G. H., Debey, P., & Gunsalus, I. C. (1977) *Eur. J. Biochem. 77*, 479.

Lang, R., Debey, P., & Gunsalus, I. C. (1979) *Eur. J. Biochem. 70* (in press).

Orrenius, S., & Ernster, L. (1974) in *Molecular Mechanisms of Oxygen Activation* (Hayaishi, O., Ed.) p 215, Academic Press, New York.

Pederson, T., & Gunsalus, I. C. (1975) in *Microsomes and Drug Oxidations* (Ullrich, V., Ed.) p 275, Pergamon Press, New York.

Pierson, W., & Cinti, D. (1977) *Biochem. Biophys. Res. Commun. 78*, 1139.

Sharrock, M., Munck, E., Debrunner, P. G., Marshall, V., Lipscomb, J. D., & Gunsalus, I. C. (1973) *Biochemistry 12*, 258.

Sligar, S. G. (1976) *Biochemistry 15*, 5399.

Sligar, S. G., & Gunsalus, I. C. (1974) *Proc. Natl. Acad. Sci. U.S.A. 71*, 3906.

Sligar, S. G., & Gunsalus, I. C. (1976) *Proc. Natl. Acad. Sci. U.S.A. 73*, 1078.

Sober, H., Ed. (1970) *Handbook of Biochemistry*, The Chemical Rubber Company, Cleveland, OH.

Tsai, R., Yu, C., Gunsalus, I. C., Peisach, J., Blumberg, W., Orme-Johnson, W., & Beinert, H. (1970) *Proc. Natl. Acad. Sci. U.S.A. 66*, 1157.

Weber, G. (1975) *Adv. Protein Chem. 29*, 1.